

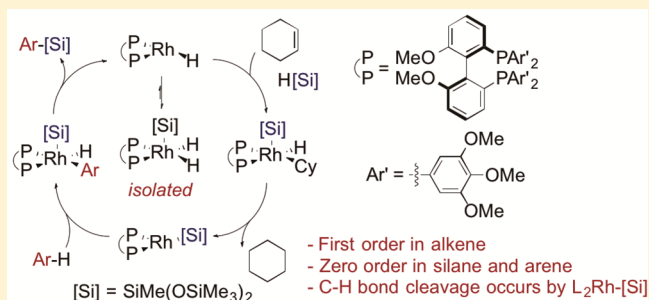
Mechanism of the Rhodium-Catalyzed Silylation of Arene C–H Bonds

Chen Cheng and John F. Hartwig*

Department of Chemistry, University of California, Berkeley, California 94720, United States

S Supporting Information

ABSTRACT: Mechanistic studies on the rhodium-catalyzed silylation of arene C–H bonds are reported. The resting state of the catalyst was fully characterized by NMR spectroscopy and X-ray diffraction and was determined to be a phosphine-ligated Rh(III) silyl dihydride complex (**I**). Results from kinetic analysis, stoichiometric reactions of isolated complexes, deuterium labeling, and kinetic isotope effects are consistent with a catalytic cycle comprising hydrogenation of the hydrogen acceptor (cyclohexene) to generate a Rh(I)–silyl species, followed by C–H activation of the arene by this Rh(I)–silyl species. After oxidative addition of the C–H bond in this mechanism, reductive elimination of the C–Si bond occurs to generate the silylarene product. The rate-limiting step (RLS) in the catalytic cycle is not the oxidative addition of an arene C–H bond; rather, it appears to be the reductive elimination of cyclohexane during the hydrogenation process. The influence of the electronic properties of the arene substituents on the reversibility and relative rates for individual steps of the mechanism, and on the regioselectivity of the C–H bond cleavage and functionalization, is reported.



INTRODUCTION

The catalytic functionalization of C–H bonds with main-group reagents has become a widely used synthetic methodology.¹ Our group has published extensively on the borylation of C–H bonds, including the mechanism of the borylation of alkyl and aryl C–H bonds with rhodium and iridium catalysts, respectively.² We recently reported the rhodium-catalyzed silylation of arenes with HSiMe(OSiMe₃)₂ (–SiMe(OSiMe₃)₂ = [Si]) that occurs under mild conditions (45 °C) with high regioselectivity derived from the steric properties of substituents on the substrates and on the ligands. This reaction forms synthetically versatile silylarene products in good yields with near-equal stoichiometry of the reaction partners.³

Methods for the silylation of arenes and alkanes have been reported, but most reactions that have been studied are intramolecular or are facilitated by a directing group. For example, our group and the Takai group reported the iridium- and rhodium-catalyzed intramolecular silylation of the C–H bonds in arenes and alkanes.⁴ In addition, various research groups have reported the silylation of arenes directed by a coordinating group on the arene. The latter reactions result in functionalization of the C–H bonds *ortho* to the directing group.⁵

Prior to our recent report, undirected, intermolecular C–H silylation of arenes had only been achieved with a large excess of arene and at high temperatures (>110 °C).⁶ The excess arene limited the synthetic utility of intermolecular silylation. In addition, few detailed mechanistic investigations had been conducted on dehydrogenative silylations;^{5c} no silyl complex has been isolated that reacts with arenes alone to form arylsilanes. Tilley and co-workers reported a bipyridine-ligated

silyliridium(III) phenyl complex that undergoes C–Si reductive elimination to generate silylbenzene, but this complex does not catalyze the silylation of arene C–H bonds.⁷

Herein, we report results of a mechanistic investigation of our rhodium-catalyzed silylation of arene C–H bonds. These results provide concrete information on the individual steps of the catalytic cycle and reveal differences between this silylation reaction and the seemingly related borylation of aryl C–H bonds. Our studies indicate that the rate-limiting step (RLS) of the catalytic cycle is not the cleavage of an arene C–H bond, as it is during the borylation of C–H bonds.⁸ Instead, hydrogenation of the hydrogen acceptor is rate limiting. We also show that C–H bond cleavage of electron-poor arenes is reversible and that the regioselectivity-determining step of the reactions of these arenes is the C–Si bond-forming reductive elimination, not arene C–H bond cleavage.

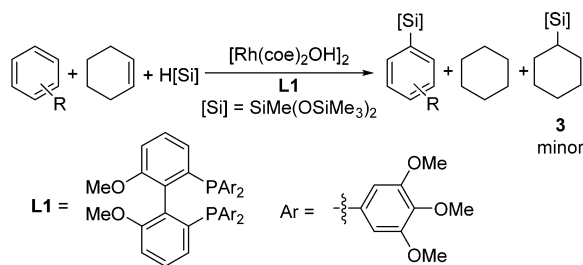
RESULTS AND DISCUSSION

The silylation of arenes under investigation occurs with a hydrosilane as the silicon source and cyclohexene as the hydrogen acceptor (Scheme 1). No arylsilane product was observed in the absence of the hydrogen acceptor. Thus, the hydrogen acceptor is intimately associated with the catalytic cycle, and the mechanism of the reaction seems likely to comprise two connected stages: dehydrogenative coupling to form the C–Si bond and hydrogenation of cyclohexene. To elucidate the individual steps of the catalytic process, we sought to identify the catalyst resting state, the kinetic behavior of the

Received: June 10, 2014

Published: July 31, 2014

Scheme 1. Rhodium-Catalyzed Silylation of Arenes

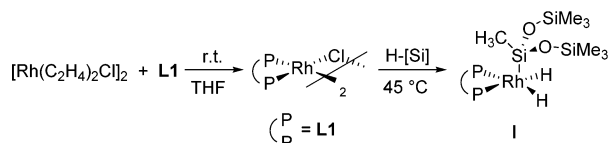


reactions, and the relative rates for reactions of different arenes. We used deuterium labeling and kinetic isotope effects to reveal the reversibility of C–H bond cleavage steps. These experiments and the implication of the results of these experiments are described in the following sections.

Identification of the Catalyst Resting State. Monitoring of a silylation reaction between $\text{HSiMe}(\text{OTMS})_2$ and 1,3-bis(trifluoromethyl)benzene (**1**) with cyclohexene as the hydrogen acceptor in THF at 45 °C revealed a discrete phosphine-ligated rhodium species. A doublet at 43.0 ppm with a $J_{\text{Rh-P}}$ value of 131 Hz was observed in the ^{31}P NMR spectrum. A hydride signal at –8.0 ppm that possessed a triplet of doublets splitting pattern ($J_{\text{Rh-H}} = 23.6$ Hz, $J_{\text{P-H}} = 44.0$ Hz) was observed in the ^1H NMR spectrum.

A rhodium complex for which the spectral data were identical to those of the complex observed during catalytic reactions was prepared independently. The complex was prepared by adding H[Si] to $[(\text{L1})\text{RhCl}]_2$ formed by the combination of $[\text{Rh}(\text{C}_2\text{H}_4)_2\text{Cl}]_2$ and **L1** at 25 °C (Scheme 2).⁹ After heating at 45 °C for 3 h, the product was isolated as a light orange solid in 82% yield.

Scheme 2. Generation of the Catalyst Resting State



On the basis of the ^1H NMR spectrum, we proposed that this complex is the Rh(III) silyl dihydride **I**. The hydride signal was observed with an intensity corresponding to two hydrogens, and three peaks corresponding to the SiCH_3 and the two diastereotopic $\text{OSi}(\text{CH}_3)_3$ groups of the silyl group were observed with proportional intensities of 3:9:9. A spin correlation between these three ^1H NMR signals and three peaks in the ^{29}Si NMR spectrum was established by a $\{^{29}\text{Si}-^1\text{H}\}$ -HMBC experiment (Figure S1, Supporting Information). Further evidence supporting this structural assignment in solution was obtained from ESI-HRMS analysis (Figure 1).

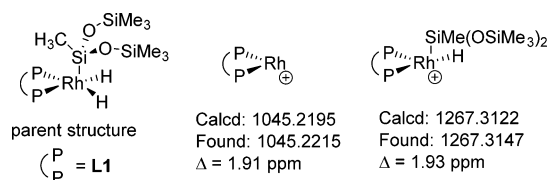


Figure 1. ESI-HRMS analysis of the resting state complex.

Complex **I** was also characterized in the solid state by single-crystal X-ray diffraction (Figure 2). Complex **I** contains a

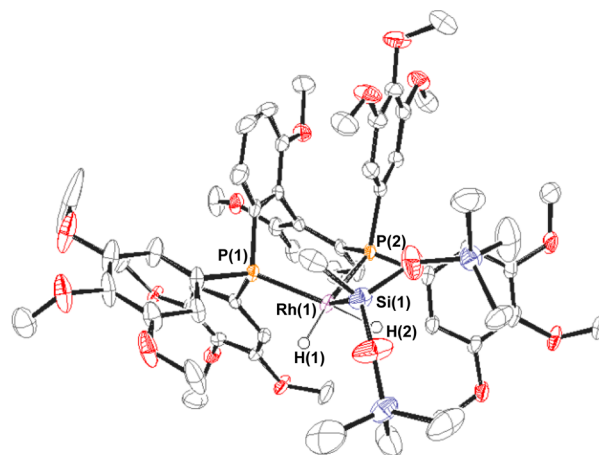


Figure 2. ORTEP diagram of **I** (thermal ellipsoids at the 50% probability level). Hydrogen atoms, except for the rhodium hydrides, are omitted. Selected bond lengths (Å): Rh1–P1 = 2.3119, Rh1–P2 = 2.3391, Rh1–H1 = 1.5269, Rh1–H2 = 1.5138, Rh1–Si1 = 2.2625, Si1–H2 = 1.9523, Si1–H1 = 2.2375. Selected bond angles (deg): P1–Rh1–Si1 = 123.4, P2–Rh1–Si1 = 109.1, H1–Rh1–Si1 = 69.3, H2–Rh1–Si1 = 58.3.

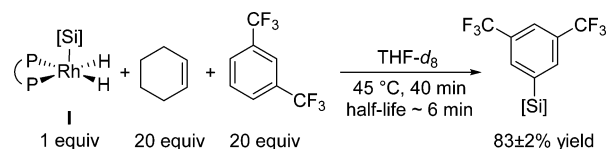
distorted square-based-pyramidal geometry in which two phosphorus atoms and two hydrides form the square base and the silyl group occupies the axial position. The distortion from a square-based pyramid is revealed by the hydride–rhodium–silicon angles, which are much smaller than the idealized 90°. The two angles are 69 and 58°, and the distances between the silicon and two hydrides differ significantly (2.24 and 1.95 Å). We ascribe this unsymmetrical ligand arrangement to the different steric environment in four quadrants created by the C_2 -symmetrical ligand and a bonding interaction between the silicon and one of the two hydrides.¹⁰

The short distance between the silicon and one of the hydrides (1.95 Å) suggests that Si–H reductive elimination should be facile. In agreement with this assertion, subjection of **I** to excess D[Si] at room temperature led to rapid and quantitative incorporation of deuterium into the hydride positions.

Because of the unequal silicon–hydride distances, the two hydrides and two phosphorus atoms are inequivalent in the solid state.¹¹ However, the two phosphorus atoms and the two rhodium–hydride protons in **I** are equivalent in solution on the NMR time scale. One hydride and one phosphorus signal were observed in the NMR spectra at room temperature. Complex **I** likely undergoes pseudorotation of the ligands in solution, and this pseudorotation allows the two metal–hydride protons and the two phosphorus atoms to undergo site exchange.

Evaluation of the Kinetic Competency of **I.** The kinetic relevance of complex **I** was investigated by both stoichiometric and catalytic reactions. Heating **I** with 20 equiv of 1,3-bis(trifluoromethyl)benzene (**1**) and 20 equiv of cyclohexene at 45 °C in THF afforded the silylarene product in $83 \pm 2\%$ yield in 40 min with a half-life of ~ 6 min (Scheme 3). This reaction is the first of an isolated silyl complex with an arene to form an arylsilane product without added silane.

The profiles of the reactions of silane with the same arene (**1**) catalyzed by isolated **I** and by the catalyst generated in situ

Scheme 3. Stoichiometric Silylation of **1** with Complex **I**

from $[\text{Rh}(\text{coe})_2\text{OH}]_2$ and **L1** are shown in Figure 3. The similarity of these two curves suggests that **I** is likely an

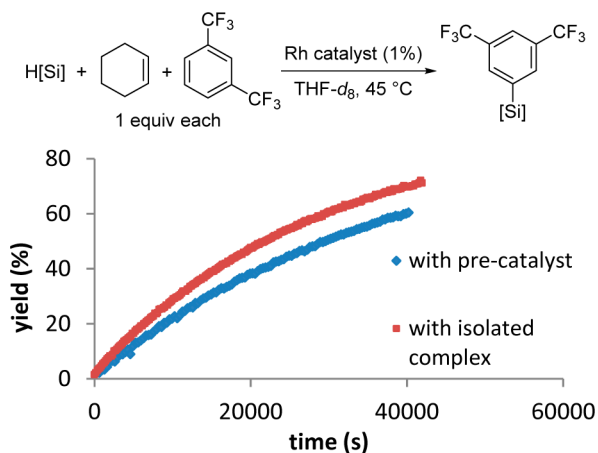


Figure 3. Reaction profiles for the silylation of 1,3-bis-(trifluoromethyl)benzene (**1**) catalyzed by **I** and the catalyst generated in situ.

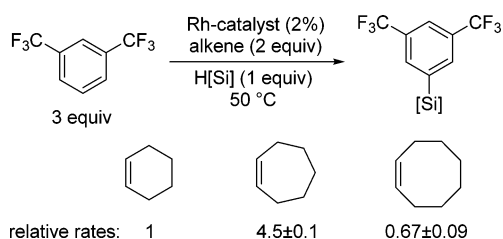
intermediate in the catalytic cycle or can enter the catalytic cycle through a low-barrier process. The downward curvature of the reaction profiles suggests a dependence of the reaction rate on the concentration of at least one of the reagents.

Determination of the Experimental Rate Law. The rate law of the catalytic silylation of **1** was determined by the method of initial rates (up to 10% conversion). The mass balance was good (Figure S3, Supporting Information); the rate of formation of the product equaled the rate of consumption of the arene. The concentration of each reagent was varied over 1 order of magnitude. Our results indicate that the reaction is first order in the concentrations of the catalyst and cyclohexene and zero order in the concentrations of the silane and the arene (Figure S4, Supporting Information).¹² Because the resting state does not contain an arene or an aryl group, the zero-order dependence of the reaction rate on the concentration of arene implies that reaction of the arene, presumably by C–H bond cleavage, occurs after the overall RLS.

On the other hand, the first-order dependence of the rate on the concentration of alkene implies that the reaction of the alkene occurs before or during the RLS. To further assess this conclusion, the initial rates of reactions run with different alkene-based hydrogen acceptors were measured (Scheme 4). The results showed that the identity of the alkene significantly influences the reaction rates. This result is consistent with a RLS involving the alkenes.

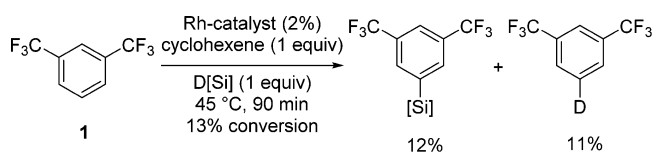
Eyring analysis of the reaction rate (Figure S5, Supporting Information) in the temperature range 308–333 K revealed overall activation parameters of $\Delta H^\ddagger = 22.4 \pm 0.5 \text{ kcal mol}^{-1}$ and $\Delta S^\ddagger = 1.5 \pm 1.6 \text{ cal mol}^{-1} \text{ K}^{-1}$. The small ΔS^\ddagger value suggests that there is no significant change in the molecularity from the ground state to the highest-energy transition state.

Scheme 4. Relative Initial Rates of Reactions Run with Different Hydrogen Acceptors



Measurement of Kinetic Isotope Effects. To assess when the C–H activation of arenes occurs in the catalytic cycle, the rates of the reactions of toluene and toluene- d_8 were measured with the two arenes in separate vessels and in the same vessel. A KIE close to unity (1.3) was observed for reactions with the two arenes in separate vessels, but a primary KIE (5.1) was observed when the two arenes were contained in the same vessel. These results suggest that cleavage of the C–H bond in toluene during the catalytic silylation process is irreversible but is not the rate-limiting step. In addition, a small KIE of 1.0 was observed for the reactions of 1,3-bis-(trifluoromethyl)benzene (**1**) and 5-D-1,3-bis(trifluoromethyl)benzene (**1-d**) in separate vessels, but the KIE from reaction of these labeled and unlabeled arenes in the same vessel was 2.9 (see the Supporting Information). Because the KIE from the competition experiment with the electron-poor arene **1** is smaller than that from the competition reaction of toluene and toluene- d_8 , C–H bond cleavage of the electron-poor arene **1** could be partially reversible.¹³

Deuterium-Labeling Experiments. To further assess the potential reversibility of the C–H bond cleavage step, the electron-poor arene **1** was allowed to react with $\text{D}[\text{Si}]$ under the standard conditions for the catalytic silylation process. Analysis of the reaction mixture after 13% conversion revealed the incorporation of deuterium into cyclohexene, cyclohexane, and the starting arene (Scheme 5). These results suggest that

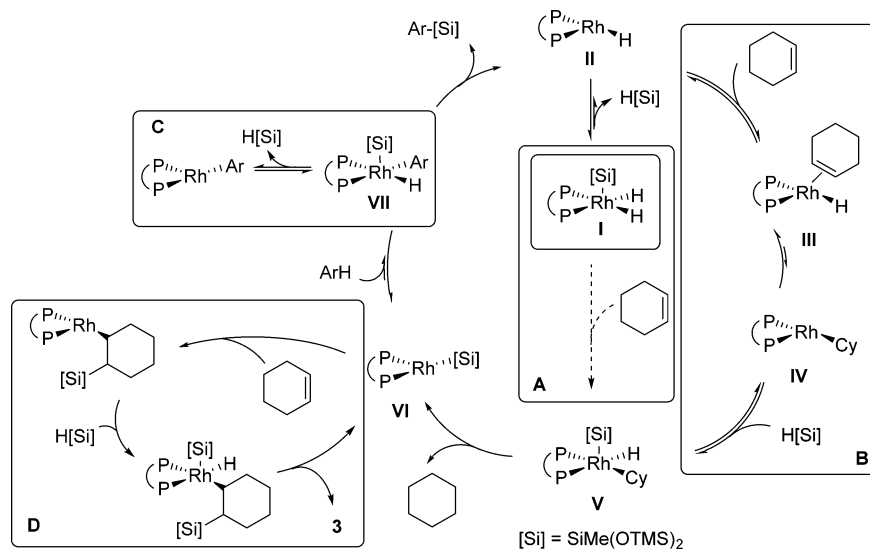
Scheme 5. Reaction of **1** with $\text{D}[\text{Si}]$ 

insertion of cyclohexene into a rhodium hydride is reversible and that cleavage of the C–H bond in **1** is partially reversible. These results are consistent with a KIE of ~ 2.9 from the competition experiment.¹⁴

In contrast to these reactions of the electron-poor arene **1**, reaction of toluene or *m*-xylene (**2**) with $\text{D}[\text{Si}]$ did not lead to incorporation of deuterium into the starting arene, even at full conversion. This result is consistent with irreversible C–H bond cleavage and a large primary competition KIE (5.1) for the reactions of toluene and toluene- d_8 in the same vessel. The effect of the electronic properties of the arene on the reversibility of the C–H activation step will be discussed in more detail later in this paper.

Proposed Mechanism. On the basis of the results above, we propose that the Rh-catalyzed silylation of arenes occurs by the pathway shown in Scheme 6. Hydrogen transfer from rhodium silyl dihydride **I** to cyclohexene generates the rhodium

Scheme 6. Proposed Mechanism for the Silylation of Arenes



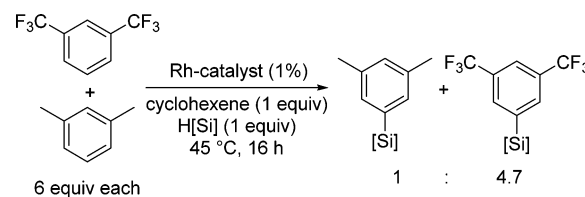
silyl intermediate VI, and this intermediate reacts with the arene to generate the rhodium(III) silyl aryl hydride complex VII. Complex VII undergoes reductive elimination to form the C–Si bond in the silylarene product and the rhodium(I) hydride II. Oxidative addition of H[Si] to II regenerates the catalyst resting state I.

Mechanism of the Cyclohexene Hydrogenation. Two major pathways are plausible for the hydrogenation of cyclohexene. Cyclohexene could bind directly to the resting state I and undergo insertion into the Rh–H bond to generate rhodium cyclohexyl silyl hydride V (Scheme 6, pathway A). Alternatively, I could undergo reversible reductive elimination of the silane to form the rhodium(I) hydride II. The release of H[Si] from I is supported by the rapid H–D exchange between free silane and I at room temperature. The rhodium(I) hydride II then binds cyclohexene and undergoes reversible insertion of the alkene into the Rh–H bond (pathway B). Readdition of H[Si], followed by C–H bond-forming reductive elimination, gives cyclohexane and rhodium silyl VI. Finally, an associative displacement of the silane by cyclohexene could take place that generates III directly from I. We were not able to experimentally distinguish among these pathways, because all are consistent with the KIE's and the experimental rate law, but we disfavor pathway A on the basis of DFT calculations we conducted on the binding of cyclohexene to I' (PAr₂ = PPh₂; [Si] = SiMe₃), a model of complex I. We were unable to locate a stable structure with cyclohexene bound to the model complex I' (pathway A). Any alkene complex structure used to initiate the calculations spontaneously dissociated the free alkene to generate I'. For details of these calculations, see the Supporting Information.

Mechanism of C–H Bond Cleavage and Arylsilane Formation. We propose that the silylarene product is generated by oxidative addition of the arene C–H bond to intermediate VI to form silyl aryl hydride complex VII, followed by reductive elimination to form the C–Si bond. No formation of product was observed in the absence of cyclohexene, a result that suggests that the rhodium silyl dihydride I does not cleave the arene C–H bonds. Instead, removal of both hydrides by the hydrogen acceptor occurs prior to C–H bond cleavage.

The effect of the electronic properties of the arenes on the rate of C–H bond cleavage was investigated. The reaction of 6 equiv of 1,3-bis(trifluoromethyl)benzene (1) and *m*-xylene (2) in the same vessel formed the two silylarene products in a ratio of 4.7:1, respectively (Scheme 7). The faster cleavage of the C–

Scheme 7. Competition Experiment between 1 and 2



H bonds of more electron-deficient arenes by rhodium silyl VI is inconsistent with an electrophilic metalation pathway and suggests that a transfer of electron density from the metal to the arene occurs during C–H bond cleavage. Similar relative rates for catalytic C–H functionalization of electronically distinct arenes have been documented.^{1b,2a} We stress, however, that the initial rates of the catalytic silylation of 1 and 2 in separate vessels are similar (1 vs 2 = 1.2:1). These similar rates are consistent with the assertion that arene C–H bond cleavage occurs after the overall RLS.

We propose that reductive elimination to form the arylsilane and rhodium hydride II occurs after C–H bond cleavage. Hydride II can bind cyclohexene to initiate the next catalytic cycle (pathway B) or react with H[Si] to afford the resting state I.

Reversibility of Arene C–H Oxidative Addition. The results from deuterium-labeling experiments showed that cleavage of the aryl C–H bonds is irreversible for reactions of electron-rich arenes and reversible for reaction of electron-deficient arenes. This difference in the reversibility of C–H bond cleavage for arenes possessing different electronic properties indicates that, for the reactions of electron-rich arenes, the transition state for C–H bond-forming reductive elimination from VII to form VI (reverse of the C–H oxidative addition step) lies at higher energy than the transition state for reductive elimination to form the C–Si bond in the arylsilane product (Figure 4, solid

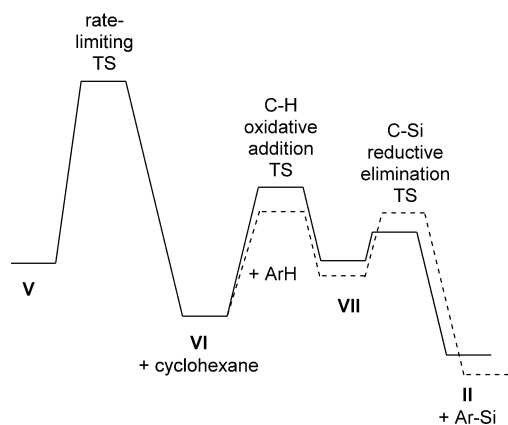


Figure 4. Qualitative free energy diagram for steps involving arenes. The solid line represents reaction with electron-rich arenes; the dashed line represents reaction with electron-deficient arenes.

line). In contrast, for the reactions of electron-poor arenes, the transition state for C–H bond-forming reductive elimination from VII to form VI lies at an energy similar to that of the transition state for reductive elimination to form the C–Si bond in the arylsilane product (Figure 4, dashed line).^{15,16}

Mechanism for the Incorporation of Deuterium into the Arene. We deduced the reversibility of arene C–H oxidative addition from the exchange of deuterium between the silane and arenes. To account for this exchange, we invoke a

mechanism in which rhodium aryl silyl hydride complex VII undergoes reversible exchange with free silane (Scheme 6, pathway C). This exchange allows deuterium to be incorporated into VII from the free deuterated silane. We propose that the reductive elimination of silane ($\text{H}[\text{Si}]$) occurs by a pathway similar to the exchange of silane with silyl dihydrido I. However, the exchange of deuterated silane into I cannot lead to deuterium incorporation into the arene, because this complex does not cleave arene C–H bonds in the absence of the cyclohexene hydrogen acceptor, which removes both hydrides to form VI.¹⁷

Consistent with the assertion that silane rapidly dissociates from VII, DFT calculations suggest that the ground-state structure of VII' ($\text{PAr}_2 = \text{PPh}_2$; $[\text{Si}] = \text{SiMe}_3$; arene = benzene), a model of complex VII, is similar to that of I'. In this structure, the silyl and the hydride groups occupy the same quadrant and the aryl group occupies the opposite quadrant of the structure of VII' (Figure 5). The proximity of the silyl and hydride ligands in the model complex VII' ($\text{Si}-\text{H} = 1.74 \text{ \AA}$, bond order 0.4467) suggests that H–Si elimination from VII and exchange with free silane is likely to occur faster than C–Si reductive elimination from VII.

Identification of the Rate-Limiting Step (RLS). Our data imply that the RLS involves a reaction between the rhodium and the alkene. The small difference in the initial rates of reactions of protio- and deuterioarenes and the zero-order dependence of the reaction rate on the concentration of arene

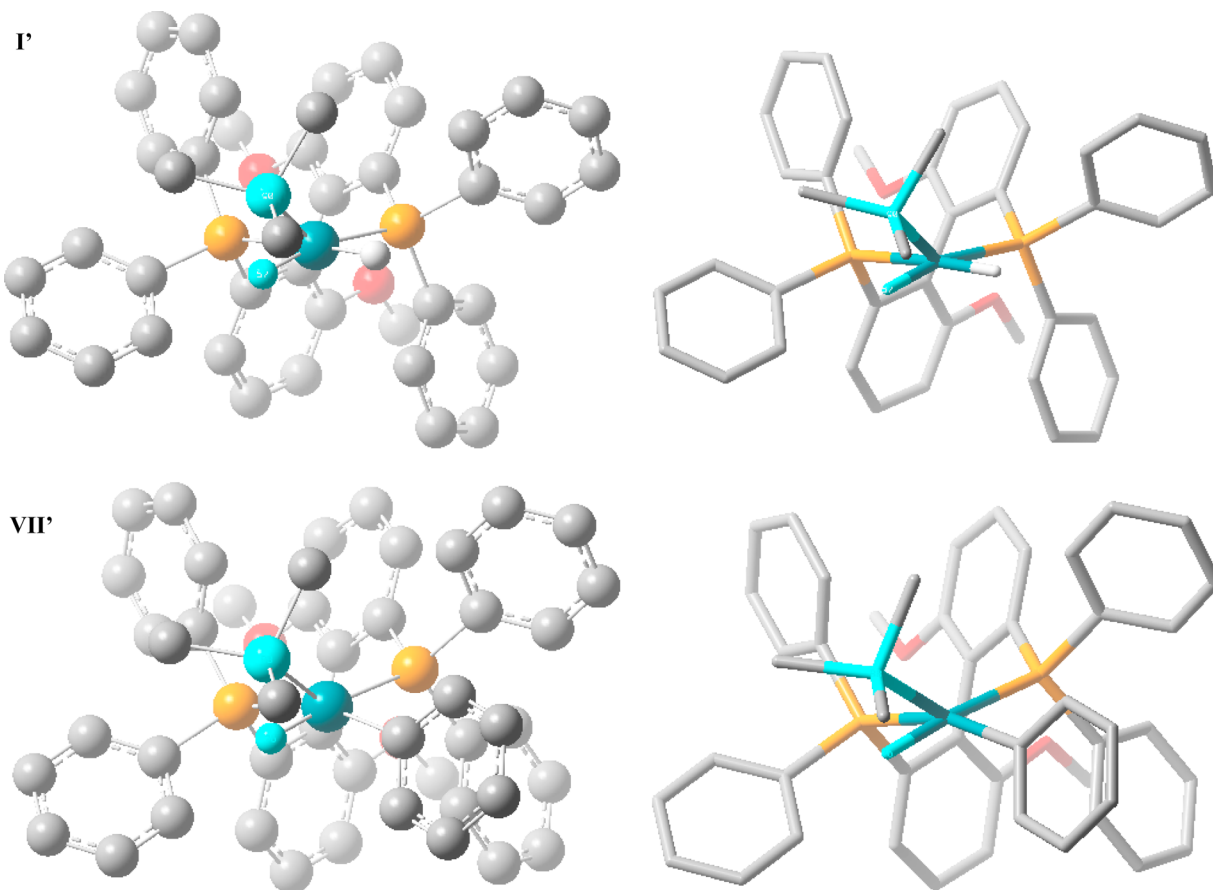


Figure 5. Comparison of the DFT-optimized ground-state structures of model complexes I' (rhodium silyl dihydride, $\text{PAr}_2 = \text{PPh}_2$, $[\text{Si}] = \text{SiMe}_3$) and VII' (rhodium silyl phenyl hydride). The silicon and hydrogen atoms with bonding interactions are highlighted in cyan. Nonessential hydrogen atoms are omitted for clarity. Color code: P, orange; O, red; Rh, dark teal.

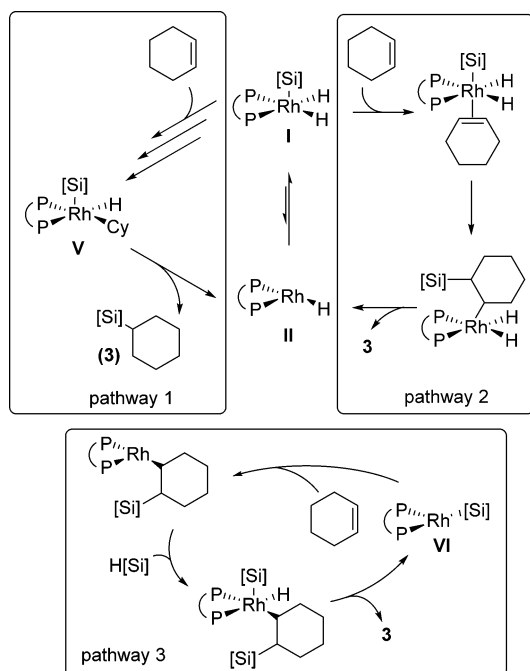
indicate that the arene C–H bond cleavage occurs after the RLS. The first-order dependence of the reaction rate on the concentration of cyclohexene implies that the hydrogen acceptor reacts prior to or during the RLS. Furthermore, the H–D exchange between cyclohexene and D[Si] suggests that reaction of the cyclohexene with the rhodium, presumably by insertion of the alkene into a Rh–H bond, occurs reversibly.

Because two major pathways (A and B, Scheme 6) were proposed for cyclohexene hydrogenation, the RLS for each pathway was analyzed. For pathway A in which cyclohexene inserts directly into the Rh–H bond of **I**, reductive elimination of cyclohexane, which occurs between cyclohexene insertion and arene C–H bond cleavage, is the RLS.

For pathway B, either oxidative addition of H[Si] to rhodium cyclohexyl **IV** or reductive elimination of cyclohexane from **V** could be rate limiting. To probe whether oxidative addition of H[Si] is the RLS, the initial rates of reactions of **3** with H[Si] and D[Si] were measured. A KIE of unity was obtained,¹⁸ which, combined with a small overall ΔS^\ddagger , suggests that addition of H–Si to **IV** is unlikely to be the RLS. Thus, for both pathways A and B, the C–H bond-forming reductive elimination from **V** to release cyclohexane is the RLS.

Mechanism for the Formation of Silylcyclohexane and Effect of Ligand Electronic Properties on Arene vs Alkene Silylation. During arene silylation, silylcyclohexane ($C_6H_{11}SiMe(OSiMe_3)_2$) (**3**) from hydrosilylation of cyclohexene formed as a minor product (Scheme 1). Hydrosilylation of alkenes is known to be catalyzed by many rhodium complexes.¹⁹ Several pathways could account for the formation of the hydrosilylation side product **3**. The silylcyclohexane could form (1) by C–Si reductive elimination from **V** (Scheme 8, pathway 1) instead of C–H reductive elimination from **V** in the productive catalytic cycle (Scheme 6), (2) by insertion of cyclohexene into the Rh–Si bond of **I** (instead of the Rh–H bond of **I** as occurs during the productive pathway),²⁰ followed by C–H bond-forming reductive elimination (Scheme 8, pathway 2), or (3) by insertion of cyclohexene into the Rh–

Scheme 8. Possible Pathways for the Formation of **3**



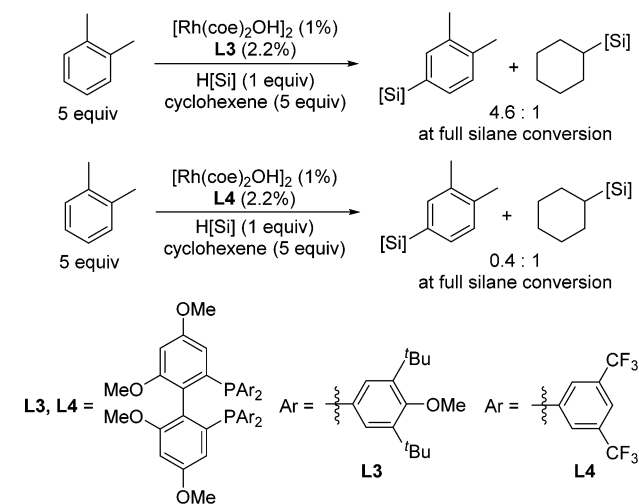
Si bond of **VI**, followed by oxidative addition of a second silane and C–H reductive elimination to regenerate **VI** (Scheme 6, pathway D, shown in Scheme 8 as pathway 3).

Pathway 3 differs from pathways 1 and 2 in that silylcyclohexane **3** cannot be generated by pathway 3 without free silane in solution; one hydrogen of **3** originates from a second molecule of silane. When rhodium silyl dihydride **I** was allowed to react with 30 equiv of cyclohexene in the absence of free silane, only cyclohexane was generated; no silylcyclohexane (**3**) was observed. This result is consistent with pathway 3 and is inconsistent with pathways 1 and 2.

In addition, pathway 1 is unlikely because intermediate **V** would more likely undergo reductive elimination to form a C–H bond (i.e., as in the normal catalytic cycle) rather than reductive elimination to form a C–Si bond. This is because rhodium-catalyzed hydrosilylation usually proceeds through insertion of the alkene into the rhodium–silicon bond, followed by reductive elimination to form the C–H bond (modified Chalk–Harrod mechanism).²¹ DFT calculations have shown that the C–Si bond-forming reductive elimination from Rh(III) has a very high barrier.^{21b}

Because rhodium silyl **VI** is the common intermediate for arene C–H activation and alkene hydrosilylation, and because insertion of alkenes into metal–silyl or metal–hydride bonds is usually favored by electron-deficient metal centers, while C–H oxidative addition is usually favored by electron-rich metal centers, perturbation of the electronic properties of the ligands should alter the ratio of hydrosilylation to arene-silylation products. Consistent with this hypothesis, the reaction of *o*-xylene with H[Si] and cyclohexene catalyzed by [Rh-(coe)₂(OH)]₂ and **L3** as ligand led to a 4.6:1 ratio of products from arene-silylation and hydrosilylation (Scheme 9), whereas

Scheme 9. Effect of Ligand on the Product Distribution



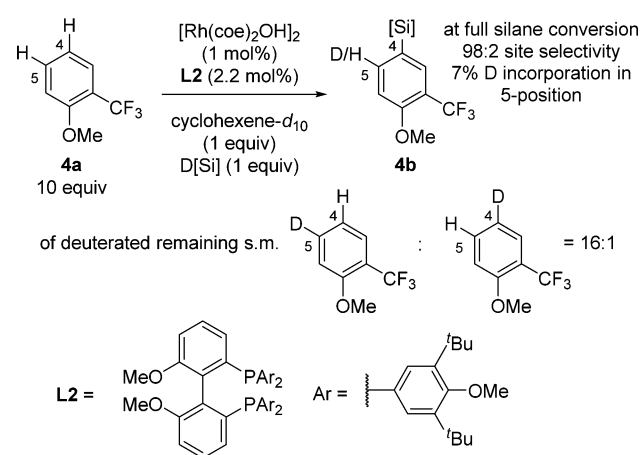
the reaction in the presence of the catalyst generated from the more electron deficient ligand **L4** produced much more product from hydrosilylation (0.4:1 arene silylation to hydrosilylation).

Origin of the Electronic Effect on Regioselectivity. In our initial report of arene silylation, we reported that the silylation of arenes occurs with regioselectivity derived from the steric effect of substituents *meta* to reactive C–H bonds. The silylation reactions of *ortho*-disubstituted arenes containing two electronically similar substituents occurred selectively at the C–

H bond located further from the larger of the two groups.³ However, the silylation of 2-(trifluoromethyl)anisole (**4a**) occurred at the position *meta* to the CF₃ group (4-position),²² which is the C–H bond closer to the larger of the two substituents.^{23,24} In this case, the silylation results from functionalization at the C–H bond that is typically less reactive toward C–H bond cleavage.^{25,26}

To assess whether the electronic effect on site selectivity results from an irreversible, kinetic selectivity from C–H bond cleavage or reversible C–H bond cleavage and irreversible C–Si bond formation, we conducted a deuterium-labeling experiment with D[Si]. The reaction of D[Si] with 10 equiv of 2-(trifluoromethyl)anisole (**4a**) and 1 equiv of cyclohexene-*d*₁₀ formed product **4b** with a selectivity of 98:2, favoring the product in which the silyl group was installed at the 4-position. Most important for understanding the origin of regioselectivity, 7% deuterium incorporation was found at the 5-position of the arylsilane product, and the ratio of deuterium incorporation into the 5-position vs the 4-position in the remaining arene was 16:1 favoring deuteration *para* to the CF₃ group (Scheme 10).

Scheme 10. Reaction of 2-(Trifluoromethyl)anisole with D[Si]



These results imply that C–H activation is reversible at both the 4- and 5-positions. C–H bond cleavage is faster at the more electron deficient 5-position (rate ~16:1), but reductive elimination is faster (and occurs almost exclusively) from the complex in which Rh is bound to the more electron rich 4-position on the arene.^{27,28} Thus, the regioselectivity of the silylation of **4a** is determined by a combination of reversible oxidative addition of the C–H bond and irreversible reductive elimination to form the C–Si bond.²⁹

CONCLUSIONS

The synthesis of Rh–silyl complexes and kinetic measurements have allowed us to propose a catalytic cycle for the silylation of arenes that is grounded in detailed experimental observations. The identification of the silylrhodium dihydride resting state, the rate law, and the influence of the electronic properties of substituents on the reaction rate and site selectivity have allowed us to pinpoint the identity and order of bond cleavages and bond formations that occur during the catalytic cycle and to identify the rate-limiting and selectivity-determining steps. With the resting state as the starting point, hydrogenation of cyclohexene is the RLS. This step precedes cleavage of the

arene C–H bond by a bisphosphine-ligated Rh(I) silyl intermediate.

(1) The catalyst resting state is the unusual five-coordinate silyl rhodium complex **I**. Complex **I** contains four sterically differentiated quadrants as a result of the C₂-symmetric ligand and the pseudoaxial silyl group. The silyl group is located in one of the two less sterically hindered quadrants and is close in distance (1.95 Å) to one of the hydride ligands. The short Si–H distance leads to facile and reversible elimination of the silane.

(2) Complex **I** is the first isolated silyl complex that reacts with arenes to form arylsilanes in both single-turnover and catalytic reactions. Complex **I** does not react directly with arenes. Instead, complex **I** reacts with the combination of cyclohexene and arenes to form cyclohexane and arylsilane. The requirement of cyclohexene implies that the cyclohexene reacts with **I** to form a species that reacts with the arene. This reaction is likely transfer of the two hydrogens to form cyclohexane and to form the bis-phosphine-ligated silyl Rh(I) complex **VI**, which cleaves the C–H bond of the arene to form a hydrido aryl silyl intermediate.

(3) DFT calculations of the structure of **VII'**, a model for the silyl aryl hydride intermediate **VII**, suggest that **VII** adopts a structure that is similar to that of **I** in which the silyl and hydride ligands occupy the same quadrant and the aryl group occupies the opposite quadrant. This type of ligand arrangement is consistent with the observed relative rate of C–Si and H–Si reductive elimination from rhodium silyl aryl hydride **VII**. Our data imply that complex **VII** undergoes rapid exchange with silane to give rise to H–D exchange between the arene and the silane; reductive elimination from **VII** to form the C–Si bond appears to be slower than the exchange of free silane with **VII**.

(4) The catalytic cycle features an unusual rate-limiting step. In contrast to many C–H functionalization reactions in which the C–H activation is the RLS,^{1b,8,30} our data strongly imply that reductive elimination from an alkylrhodium(III) hydride complex, a facile step in many rhodium-catalyzed alkene hydrogenation reactions,³¹ is the RLS of the arene silylation reaction.

(5) The C–H activation is reversible during reactions of electron-poor arenes and is not the regioselectivity-determining step when the regioselectivity is dominated by electronic effects. We showed that the silylation occurs preferentially at the site that undergoes C–H bond cleavage more slowly, as indicated by the relative incorporation of deuterium from deuterated silane into different sites on 2-(trifluoromethyl)anisole (**4a**). These H–D exchange data and the site selectivity for arene silylation imply that the regioselectivity-determining step is the formation of the C–Si bond. Reversible C–H activation occurs at both positions *para* to electron-donating and electron-withdrawing groups, but the product-forming reductive elimination occurs much faster from the complex containing the metal bound to the more electron-rich carbon.

(6) Hydrosilylation of the alkene hydrogen acceptor is catalyzed by the same intermediate (**VI**) that activates the arene C–H bonds. Because alkene insertion and C–H oxidative addition are usually favored by the opposite electronic properties of the metal center, the competing hydrosilylation is suppressed by using catalysts containing more electron-donating biarylphosphine ligands.

Overall, these studies show that the mechanism of the rhodium-catalyzed silylation is distinct from that of rhodium-

iridium-catalyzed borylation of arenes. C–H bond cleavage in the borylation processes occur by Rh(III) boryl and Ir(III) boryl intermediates.^{8,32} We presume that the change in rate-limiting step from generation of the reactive intermediate that cleaves the C–H bond (as in silylation) to cleavage of the C–H bond (as in borylation) is a function of the different oxidation states of the boryl and silyl complexes that cleave the C–H bonds. Cleavage of a C–H bond by a Rh(III) or Ir(III) species is likely less facile than cleavage of a C–H bond by a Rh(I) silyl species.

Extensive computational data are needed to gain information on the C–H bond cleavage step and the relationship between the main-group-assisted C–H bond cleavage reactions by boryl complexes³³ and the role of silicon in the C–H bond cleavage step of this Rh-catalyzed reaction. Such computational studies and an assessment of the effect of ligands on the individual steps as a means to create more active catalysts will be the studies of future work in our laboratory.

■ ASSOCIATED CONTENT

■ Supporting Information

Text, figures, tables, and a CIF file giving experimental procedures, computational details, kinetics data, and crystallographic information. This material is available free of charge via the Internet at <http://pubs.acs.org>.

■ AUTHOR INFORMATION

Corresponding Author

*E-mail for J.F.H.: jhartwig@berkeley.edu.

Notes

The authors declare no competing financial interest.

■ ACKNOWLEDGMENTS

We thank the NSF (CHE-1213409) for funding, the Molecular Graphics and Computation Facility (CHE-0840505) of College of Chemistry, University of California, Berkeley, for computational resources, Dr. A. DiPasquale for X-ray crystallography, and the M. B. Francis group for use of a centrifuge.

■ REFERENCES

- (1) (a) Godula, K.; Sames, D. *Science* **2006**, *312*, 67–72. (b) Lyons, T. W.; Sanford, M. S. *Chem. Rev.* **2010**, *110*, 1147–1169. (c) Jia, C.; Kitamura, T.; Fujiwara, Y. *Acc. Chem. Res.* **2001**, *34*, 633–639. (d) Ritleng, V.; Sirlin, C.; Pfeffer, M. *Chem. Rev.* **2002**, *102*, 1731–1769. (e) Kakiuchi, F.; Murai, S. *Acc. Chem. Res.* **2002**, *35*, 826–834. (f) Colby, D. A.; Bergman, R. G.; Ellman, J. A. *Chem. Rev.* **2010**, *110*, 624–655. (g) Cho, S. H.; Kim, J. Y.; Kwak, J.; Chang, S. *Chem. Soc. Rev.* **2011**, *40*, 5068–5083.
- (2) (a) Mkhali, I. A. I.; Barnard, J. H.; Marder, T. B.; Murphy, J. M.; Hartwig, J. F. *Chem. Rev.* **2010**, *110*, 890–931. (b) Hartwig, J. F. *Acc. Chem. Res.* **2013**, *45*, 864–873. (c) Waltz, K. M.; Hartwig, J. F. *Science* **1997**, *277*, 211–213. (d) Chen, H. Y.; Schlecht, S.; Sempke, T. C.; Hartwig, J. F. *Science* **2000**, *287*, 1995–1997. (e) Ishiyama, T.; Takagi, J.; Ishida, K.; Miyaura, N.; Anastasi, N.; Hartwig, J. F. *J. Am. Chem. Soc.* **2002**, *124*, 390–391. (f) Ishiyama, T.; Takagi, J.; Hartwig, J. F.; Miyaura, N. *Angew. Chem., Int. Ed.* **2002**, *41*, 3056–3058. (g) Liskey, C. W.; Hartwig, J. F. *J. Am. Chem. Soc.* **2012**, *134*, 12422–12425. (h) Liskey, C. W.; Hartwig, J. F. *J. Am. Chem. Soc.* **2013**, *135*, 3375–3378.
- (3) Cheng, C.; Hartwig, J. F. *Science* **2014**, *343*, 853–857.
- (4) (a) Simmons, E. M.; Hartwig, J. F. *J. Am. Chem. Soc.* **2010**, *132*, 17092–17095. (b) Simmons, E. M.; Hartwig, J. F. *Nature* **2012**, *483*, 70–73. (c) Ureshino, T.; Yoshida, T.; Kuninobu, Y.; Takai, K. *J. Am.*

Chem. Soc. **2010**, *132*, 14324–14326. (d) Kuninobu, Y.; Nakahara, T.; Takeshima, H.; Takai, K. *Org. Lett.* **2013**, *15*, 426–428.

(5) (a) Ihara, H.; Suginome, M. *J. Am. Chem. Soc.* **2009**, *131*, 7502–7503. (b) Kakiuchi, F.; Igi, K.; Matsumoto, M.; Chatani, N.; Murai, S. *Chem. Lett.* **2001**, *30*, 422–423. (c) Oyamada, J.; Nishiura, M.; Hou, Z. *Angew. Chem., Int. Ed.* **2011**, *50* (45), 10720–10723. (d) Williams, N. A.; Uchamaru, Y.; Tanaka, M. *J. Chem. Soc., Chem. Commun.* **1995**, 1129–1130. (e) Choi, G.; Tsurugi, H.; Mashima, K. *J. Am. Chem. Soc.* **2013**, *135*, 13149–13161.

(6) (a) Uchamaru, Y.; Sayed, A. M. M. E.; Tanaka, M. *Organometallics* **1993**, *12*, 2065–2069. (b) Ezbiatsky, K.; Djurovich, P. I.; LaForest, M.; Sinning, D. J.; Zayes, R.; Berry, D. H. *Organometallics* **1998**, *17*, 1455–1457. (c) Saiki, T.; Nishio, Y.; Ishiyama, T.; Miyaura, N. *Organometallics* **2006**, *25*, 6068–6073. (d) Ishiyama, T.; Sato, K.; Nishio, Y.; Miyaura, N. *Angew. Chem., Int. Ed.* **2003**, *42*, 5346–5348. (e) Murata, M.; Fukuyama, N.; Wada, J.-i.; Watanabe, S.; Masuda, Y. *Chem. Lett.* **2007**, *36*, 910–911.

(7) McBee, J. L.; Tilley, T. D. *Organometallics* **2009**, *28*, 5072–5081.

(8) Boller, T. M.; Murphy, J. M.; Hapke, M.; Ishiyama, T.; Miyaura, N.; Hartwig, J. F. *J. Am. Chem. Soc.* **2005**, *127*, 14263–14278.

(9) Korenaga, T.; Osaki, K.; Maenishi, R.; Sakai, T. *Org. Lett.* **2009**, *11*, 2325–2328.

(10) Natural bond orbital (NBO) analysis on the DFT-optimized ground state structure of **1'**, a simplified model (PA₂ = PPh₂; [Si] = SiMe₃) of rhodium silyl dihydride **1**, yields a bond order of 0.4211 for the Si–H bond. See the Supporting Information for details.

(11) Because the ligand is chiral, the two phosphorus atoms and two hydrides would be inequivalent, even if the silyl group assumed an idealized axial position.

(12) The silylation of 1,3-xylene is also zero order in the concentration of the arene (see the Supporting Information), suggesting that reactions of electron-rich and electron-deficient arenes occur by the same mechanism.

(13) For a quantitative estimation of the KIE for partially reversible reactions, see the Supporting Information.

(14) Deuterium exchange among the silane, cyclohexene, and 1,3-bis(trifluoromethyl)benzene (**1**) could complicate the KIE results because this process lowers the deuterium content in the starting arene. However, because the KIE experiments were conducted with excess arenes, and initial reaction rates (up to 5% conversion) were measured, the experimental results should be close to the true relative rates for reaction of 1,3-bis(trifluoromethyl)benzene and 1,3-bis(trifluoromethyl)benzene-*d*.

(15) Ozawa and co-workers have shown that the barriers for C–Si reductive elimination from Pt(II) alkynyl silyl complexes are higher for more electron deficient alkynyl groups.

(16) Ozawa, F.; Mori, T. *Organometallics* **2003**, *22*, 3593–3599.

(17) Control experiments with 1,3-bis(trifluoromethyl)benzene (**1**) run without cyclohexene (which would not generate **VI**) or without the ligand gave no silylarene product or deuterated starting arene, suggesting that neither **II** (or **I**) nor an unligated rhodium species is responsible for arene C–H activation.

(18) The reaction with D[Si] was run with cyclohexene-*d*₁₀ and 5-D-1,3-bis(trifluoromethyl)benzene to avoid erosion of the deuterium content of the silane caused by H–D exchange with cyclohexene and the arene.

(19) *Modern Rhodium-Catalyzed Organic Reactions*, 1st ed.; Wiley-VCH: Weinheim, Germany, 2005.

(20) Pathway 2 requires the alkene hydrogenation step to proceed through pathway A (Scheme 6), which we disfavor because of unfavorable binding of cyclohexene to **I**.

(21) (a) Duckett, S. B.; Perutz, R. N. *Organometallics* **1992**, *11*, 90–98. (b) Sakaki, S.; Sumimoto, M.; Fukuhara, M.; Sugimoto, M.; Fujimoto, H.; Matsuzaki, S. *Organometallics* **2002**, *21*, 3788–3802.

(22) Only the 4- and 5-positions are available for silylation. The 3- and 6-positions are not available because these C–H bonds have substituents *ortho* to them.

(23) CF₃ *A* value 2.4–2.5, MeO *A* value 0.55–0.75. The large *A* value of a trifluoromethyl group does not correctly reflect its size due to the

stereoelectronic effect. However, it is generally accepted that a trifluoromethyl group is larger than a methoxy group.

(24) Eliel, E. L.; Wilen, S. H.; Mander, L. N. *Stereochemistry of Organic Compounds*; Wiley: New York, 1994.

(25) In the iridium-catalyzed borylation of unsymmetrical 1,2-disubstituted arenes in which the C–H activation is the rate- and regioselectivity-determining step, the product distribution reflects the relative rates of C–H activation at different positions. Borylation of **4a** led to a 74:26 mixture of products favoring borylation *meta* to the MeO group (5-position), implying that C–H activation occurs preferentially at the 5- over the 4-position in a ratio of ~3:1. Similar trends have been observed in borylation of other unsymmetrical 1,2-disubstituted arenes. Both the acidity of the C–H bond and the Ir–C bond strength of the Ir–aryl complex have been invoked to explain the regioselectivity of oxidative addition.

(26) (a) Tajuddin, H.; Harrisson, P.; Bitterlich, B.; Collings, J. C.; Sim, N.; Batsanov, A. S.; Cheung, M. S.; Kawamorita, S.; Maxwell, A. C.; Shukla, L.; Morris, J.; Lin, Z.; Marder, T. B.; Steel, P. G. *Chem. Sci.* **2012**, *3*, 3505–3515. (b) Vanchura, B. A.; Preshlock, S. M.; Roosen, P. C.; Kallepalli, V. A.; Staples, R. J.; Maleczka, R. E.; Singleton, D. A.; Smith, M. R. *Chem. Commun.* **2010**, *46*, 7724–7726.

(27) Hartwig and co-workers have computed the barriers of C–B bond-forming reductive elimination in the borylation of pyridine. The barriers to reductive elimination from the more electron rich 3- and 4-positions are ~5 kcal/mol lower than the barrier to reductive elimination from the more electron deficient 2-position.

(28) Larsen, M. A.; Hartwig, J. F. *J. Am. Chem. Soc.* **2014**, *136*, 4287–4299.

(29) On the basis of the rates of C–H activation (16:1 for the 5- vs 4-position) and the product distribution (1:50 for the 5- vs 4-position), the ratio of the rates of the reductive elimination step is 1:800 favoring the 4-position. It is possible that this large ratio is not caused by the electronic effect alone, and detailed computational studies to probe the steric effect of the substituents on the rate of reductive elimination will be the focus of future studies.

(30) Gómez-Gallego, M.; Sierra, M. A. *Chem. Rev.* **2011**, *111*, 4857–4963.

(31) Oro, L. A.; Carmona, D. Rhodium. In *The Handbook of Homogeneous Hydrogenation*; de Vries, J. G.; Elsevier, C. J., Eds.; Wiley-VCH: Weinheim, Germany, 2007; pp 3–30.

(32) Hartwig, J. F.; Cook, K. S.; Hapke, M.; Incarvito, C. D.; Fan, Y.; Webster, C. E.; Hall, M. B. *J. Am. Chem. Soc.* **2005**, *127*, 2538–2552.

(33) Webster, C. E.; Fan, Y.; Hall, M. B.; Kunz, D.; Hartwig, J. F. *J. Am. Chem. Soc.* **2003**, *125*, 858–859.